Richa Sharma

ELASTIC-PLASTIC STRESSES IN A THIN ROTATING DISK OF FUNCTIONALLY GRADED MATERIAL WITH EXPONENTIALLY VARYING THICKNESS UNDER INTERNAL PRESSURE

ELASTOPLASTIČNI NAPONI U TANKOM ROTIRAJUĆEM DISKU OD FUNKCIONALNOG KOMPOZITA SA EKSPONENCIJALNOM PROMENOM DEBLJINE POD UNUTRAŠNJIM PRITISKOM

Originalni naučni rad / Original scientific paper
UDK /UDC: 66.018:539.319

Rad primljen / Paper received: 3.07.2019

Adresa autora / Author's address:
Department of Mathematics, School of Basic Sciences and Research, Sharda University, Greater Noida, India
email: richa.sharma@sharda.ac.in

Keywords
- elastic, plastic
- rotating disk
- pressure
- functionally graded material
- finite deformation

Ključne reči
- elastičan, plastičan
- rotirajući disk
- pritisak
- funkcionalni kompozitni materijal
- konačna deformacija

Abstract

Stress analysis has been performed in an elastic-plastic rotating disk made of functionally graded material. Elastic-plastic stresses are calculated by applying the concepts of transition theory based on generalized principal strain measure using Eulerian finite deformation theory. The results obtained from the analysis are discussed numerically and depicted graphically for different geometrical parameters. It is observed that variable thickness and non-homogeneity have significant effects on the circumferential stresses in the functionally graded rotating disk.

Izvod

Izvedena je naponska analiza kod elastoplastičnog rotirajućeg diska od funkcionalnog kompozitnog materijala. Elastoplastični naponi su sračunati primenom koncepta teorije prelaznih napona, na bazi principa generalisanih mera deformacije, korišćenjem Ojlerove teorije konačne deformacije. Rezultati analize su diskutovani numerički i obrađeni grafički za različite geometrijske parametre. Uočava se da promenljiva debljina i nehomogenost imaju značajan uticaj na obimske napone u rotirajućem disku od funkcionalnog kompozita.

INTRODUCTION

The design of rotating disk has been a subject of long-standing interest with useful applications such as turbines, rotors, computer disk drives etc. Functionally graded materials (FGMs) are advanced composite materials that attract attention of researchers nowadays due to their distinct mechanical properties. These materials can survive in high temperature conditions. Functionally graded rotating disks have numerous applications in different industries, such as electric motors, computers, combustion engines, etc. These structures have to work under different types of loadings such as high temperature and pressure, etc. Callioglu et al. /1/ used finite element method for solving problems related to rotating disk. Stress and strain analysis for a disk under constant rotation is done by Sharma et al. /2/ under temperature distribution by using finite element method. Kermani et al. /3/ found the solution of equations of motion for rotating plates made of functionally graded material by using the method of differential quadrature. It is observed that rotating plates made of functionally graded material have high angular speed. Zafarmand and Hassani /4/ discussed the stress in rotating thick disks of functionally graded material with variable thickness by applying finite element method. Vivio et al. /5/ performed stress analysis in rotating disk subjected to temperature along the radial direction by taking the variable thickness of the disk to be hyperbolic. They solved the governing equations by analytical methods. Rosyid et al. /6/ considered a problem of an inhomogeneous rotating disk with the thickness varying arbitrarily in the radial direction and applied the finite element method to evaluate stresses. Kouchakzadeh and Entezari /7/ simplified the governing system of equations by applying the Fourier-Bessel transform. They concluded that obtained results are compatible with available numerical results. Carrera et al. /8/ proposed a one-dimensional finite element method for stress analysis in a rotating disk of varying thickness. They compared their obtained results with the results obtained by using the finite difference method and the analytical method. Entezari and Kouchakzadeh /9/ solved the governing equations of rotating disk subjected to temperature by analytical methods using the principle of superposition and the Fourier-Bessel transform. The results of the study are compared with numerical results available in literature. Shahriari et al. /10/ studied vibrations in rotating disk by using generalized differential quadrature method. On the basis of their analysis they concluded that use of functionally graded material could decrease the value of radial stresses and decrease the value of radial displacement. Jalali et al. /11/ analysed the rotating disk of functionally graded material with variable thickness and concluded that critical speed of the functionally graded disk is increased by increasing the ratio of internal and external radii of the disk.

Borah /13/ has discussed the transition theory by employing the concept of generalized finite strain measures. Many

authors /12-28/ have implemented this theory to problems related to various types of solid structures such as cylinders, shells and disks, etc. For instance Aggarwal et al. /15/ calculated the stresses in functionally graded cylinder and found that functionally graded pressurized cylinder is better choice for designing purposes. Sharma et al. /18/ evaluated the thermal shear stresses in torsion of functionally graded cylinder under internal and external pressure. Sharma and Panchal /20/ and Sharma et al. /21/ used the concept of transition theory for evaluating the stresses in spherical shells and composite transversely isotropic cylinder, respectively. Sharma et al. /22/ analysed creep torsion in thick cylinder under internal and external pressure and concluded that functionally graded materials are better for designing purposes.

In this paper, elastic-plastic stresses are calculated in a thin rotating disk made of functionally graded material whose thickness is varying exponentially, subjected to internal pressure. The thickness h of the disk is taken in the form $h = h_0 e^{-(r/b)^m}$, where h_0 is thickness and m is a thickness parameter.

MATHEMATICAL FORMULATIONS

Consider a thin circular disk of variable thickness having internal radius a and external radius b, respectively. The angular velocity of the disk is taken as ω. The disk is thin so that it is effectively in a state of plane stress ($T_{zz} = 0$) and the variation of the thickness is radial and symmetric with respect to the mid plane. In cylindrical polar co-ordinates the displacements are given by

$$u = r(1-\beta),\ v = 0 \text{ and } w = dz \tag{1}$$

where: β is a function of $r = \sqrt{x^2 + y^2}$; and d is a constant.

The generalized components of strain are given by

$$e_{rr} = \frac{1}{n}\left[1-(r\beta'+\beta)^n\right],\ e_{\theta\theta} = \frac{1}{n}\left[1-\beta^n\right],$$
$$e_{zz} = \frac{1}{n}\left[1-(1-d)^n\right],\ e_{r\theta} = e_{\theta z} = e_{zr} = 0. \tag{2}$$

where: n is the measure; and $\beta' = d\beta/dr$.

Stress-strain relations are defined as

$$T_{rr} = \lambda[e_{rr} + e_{\theta\theta}] + 2\mu e_{rr},$$
$$T_{\theta\theta} = \lambda[e_{rr} + e_{\theta\theta}] + 2\mu e_{\theta\theta}, \tag{3}$$
$$T_{zz} = T_{zr} = T_{r\theta} = T_{\theta z} = 0.$$

The compressibility of the functionally graded cylinder is given by

$$C = C_0\left(\frac{r}{b}\right)^k \tag{4}$$

By using Eqs.(3) and (4), stresses are given as

$$T_{rr} = \frac{3}{3-2C_0\left(\frac{r}{b}\right)^k}\left[\left(2-C_0\left(\frac{r}{b}\right)^k\right)(1-\beta^n(1+p)^n) + \left(1-C_0\left(\frac{r}{b}\right)^k\right)(1-\beta^n)\right],$$
$$T_{\theta\theta} = \frac{3}{3-2C_0\left(\frac{r}{b}\right)^k}\left[\left(1-C_0\left(\frac{r}{b}\right)^k\right)(1-\beta^n(1+p)^n) + \left(2-C_0\left(\frac{r}{b}\right)^k\right)(1-\beta^n)\right]. \tag{5}$$

where: $r\beta' = \beta P$; $C = 2\mu/(\lambda + 2\mu)$.

Equation of equilibrium is

$$\frac{d}{dr}(hrT_{rr}) - hT_{\theta\theta} + \rho\omega^2 r^2 h = 0. \tag{6}$$

IDENTIFICATION OF TRANSITION POINT

According to transition theory there exists an intermediate state in between the elastic and plastic region which is called transition state. So, at transition the differential system defining the elastic state should attain some sort of criticality.

Using Eqs.(5) and (6), the nonlinear differential equation is obtained as

$$-\left(2-C_0\left(\frac{r}{b}\right)^k\right)n\beta^{n+1}(1+P)^n\left(\frac{nP}{r}\right)\frac{dP}{d\beta} = \rho r^2\omega^2 n\left(3-2C_0\left(\frac{r}{b}\right)^k\right) + rm\left[\left(2-C_0\left(\frac{r}{b}\right)^k\right)(1-\beta^n(1+P^n) + \left(1-C_0\left(\frac{r}{b}\right)^k\right)(1-\beta^n)\right] -$$
$$-\beta^n((1+P)^n+1) - \frac{6kC_0\left(\frac{r}{b}\right)^{k-1}}{b\left(3-2C_0\left(\frac{r}{b}\right)^k\right)}\left\{\left(2-C_0\left(\frac{r}{b}\right)^k\right)(1-\beta^n(1+P)^n) + \left(1-C_0\left(\frac{r}{b}\right)^k\right)(1-\beta^n)\right\} + \left(\frac{k}{b}\right)C_0\left(\frac{r}{b}\right)^{k-1}(1-\beta^n(1+P)^n) +$$
$$+\left(2-C_0\left(\frac{r}{b}\right)^k\right)\frac{nP\beta^n}{r}(1+P)^n + \left(\frac{k}{b}\right)C_0\left(\frac{r}{b}\right)^{k-1}(1-\beta^n) + \frac{nP\beta^n\left(1-C_0\left(\frac{r}{b}\right)^k\right)}{r}. \tag{7}$$

The critical/transition points from the above equation are obtained as $P \to -1$; $P \to \pm\infty$.

The boundary conditions are taken as

$$T_{rr} = -p \text{ at } r = a \text{ and } T_{rr} = 0 \text{ at } r = b. \tag{8}$$

TRANSITION FROM ELASTIC TO PLASTIC STATE

According to transition theory /12-28/, the transition from elastic to plastic state occurs at $P \to \pm\infty$. For finding transitional and fully plastic stresses, the transition function is taken as

$$R = \frac{n}{2\mu} T_{rr} + B \,. \tag{9}$$

Logarithmic differentiation of Eq.(9) with the use of Eq.(7) and transition point $P \to \pm\infty$ yields:

$$R = Ae^{mr^2/2}\left(3-2C_0\left(\frac{r}{b}\right)^k\right)^3 . \tag{10}$$

With the help of Eqs.(5), (9) and (10), the transition stresses are obtained as follows

$$T_{rr} = \frac{3Ae^{mr^2/2}\left(3-2C_0\left(\frac{r}{b}\right)^k\right)^2}{n} - \frac{3B}{n\left(3-2C_0 3-2C_0\left(\frac{r}{b}\right)^k\right)},$$

$$T_{\theta\theta} = \frac{-m}{b}\left(\frac{r}{b}\right)^{m-1}\left[3Ae^{mr^2/2}\left(3-2C_0\left(\frac{r}{b}\right)^k\right)^2 - \frac{3B}{n\left(3-2C_0\left(\frac{r}{b}\right)^k\right)}\right] - \frac{6BC_0k\left(\frac{r}{b}\right)^{k-1}}{bn\left(3-2C_0\left(\frac{r}{b}\right)^k\right)^2} + \rho r^2\omega^2 + \tag{11}$$

$$+\frac{3Ae^{mr^2/2}\left(3-2C_0\left(\frac{r}{b}\right)^k\right)}{n}\left(\left(3-2C_0\left(\frac{r}{b}\right)^k\right)mr - \frac{4C_0k\left(\frac{r}{b}\right)^{k-1}}{b}\right).$$

Using Eq.(8) in above equations we have

$$A = \frac{-p(3-2C_0(a/b)^k)n}{3[(3-2C_0(r/b)^k)^3 e^{ma^2/2} - n(3-2C_0)^3 e^{mb^2/2}]}, \quad B = \frac{-p(3-2C_0(a/b)^k)n^2(3-2C_0)^3 e^{mb^2/2}}{3[(3-2C_0(r/b)^k)^3 e^{ma^2/2} - n(3-2C_0)^3 e^{mb^2/2}]}. \tag{12}$$

By using Eqs.(11) and (12), the Tresca's yield criteria is given as

$$\left|T_{rr} - T_{\theta\theta}\right|_{r=a} = \tag{13}$$

$$= \left| \frac{-p\left(3-2C_0\left(\frac{a}{b}\right)^k\right)^3 e^{\frac{ma^2}{2}}\left(1-ma-\frac{m}{b}\left(\frac{a}{b}\right)^{m-1}+\frac{4C_0\frac{k}{b}\left(\frac{a}{b}\right)^{k-1}}{3-2C_0\left(\frac{a}{b}\right)^k}\right)+(3-2C_0)^3 e^{\frac{mb^2}{2}} p\left(1-\frac{m}{b}\left(\frac{a}{b}\right)^{m-1}-\frac{2C_0\frac{k}{b}\left(\frac{a}{b}\right)^{k-1}}{3-2C_0\left(\frac{a}{b}\right)^k}\right)}{\left(3-2C_0\left(\frac{r}{b}\right)^k\right)^3 e^{\frac{ma^2}{2}} - n(3-2C_0)^3 e^{\frac{mb^2}{2}}} - \rho a^2\omega^2 \right| = Y .$$

Effective pressure required for initial yielding is given from Eq.(13) as

$$\frac{p}{Y} = \frac{\left[\left(3-2C_0\left(\frac{r}{b}\right)^k\right)^3 e^{\frac{mr^2}{2}} - n(3-2C_0)^3 e^{\frac{mb^2}{2}}\right]\left(1+\frac{\rho\omega^2a^2}{Y}\right)}{\left[\left(3-2C_0\left(\frac{r}{b}\right)^k\right)^3 e^{\frac{mr^2}{2}}\left(1-mr-\frac{m}{b}\left(\frac{r}{b}\right)^{m-1}+\frac{4C_0\frac{k}{b}\left(\frac{r}{b}\right)^{k-1}}{3-2C_0\left(\frac{r}{b}\right)^k}\right)+(3-2C_0)^3 e^{\frac{mb^2}{2}}\left(1-\frac{m}{b}\left(\frac{r}{b}\right)^{m-1}-\frac{2C_0\frac{k}{b}\left(\frac{r}{b}\right)^{k-1}}{3-2C_0\left(\frac{r}{b}\right)^k}\right)\right]}. \tag{14}$$

As initial yielding occurs at the internal surface and thus, fully plastic state occurs at the external surface. Therefore, Eq.(11) at $r = b$ becomes

$$\left|T_{rr}-T_{\theta\theta}\right|_{r=b}=$$

$$=\left|\frac{-p\left(3-2C_0\left(\frac{a}{b}\right)^k\right)(3-2C_0)^2e^{\frac{mb^2}{2}}\left(1-ma-\frac{m}{b}\left(\frac{a}{b}\right)^{m-1}+\frac{4C_0\frac{k}{b}}{3-2C_0}\right)+(3-2C_0)^3e^{\frac{mb^2}{2}}p\left(1-\frac{m}{b}-\frac{2C_0\frac{k}{b}}{3-2C_0}\right)}{\left(3-2C_0\left(\frac{r}{b}\right)^k\right)^3e^{\frac{ma^2}{2}}-n(3-2C_0)^3e^{\frac{mb^2}{2}}}-\rho b^2\omega^2\right|=Y_1\,. \quad (15)$$

For fully plastic state ($C_0\to 0$), Eq.(15) becomes

$$\left|T_{rr}-T_{\theta\theta}\right|_{r=b}=\left|\frac{-pe^{\frac{mb^2}{2}}\left(1-ma-\frac{m}{b}\left(\frac{a}{b}\right)^{m-1}\right)+e^{\frac{mb^2}{2}}p\left(1-\frac{m}{b}\right)}{e^{\frac{ma^2}{2}}-ne^{\frac{mb^2}{2}}}-\rho b^2\omega^2\right|=Y_1\,. \quad (16)$$

Effective pressure required for fully plastic state is given

$$\frac{p}{Y_1}=\frac{\left(e^{\frac{mr^2}{2}}-ne^{\frac{mb^2}{2}}\right)\left(1+\frac{\rho b^2\omega^2}{Y_1}\right)}{e^{\frac{mr^2}{2}}\left(1-ma-\frac{m}{b}\left(\frac{a}{b}\right)^{m-1}\right)-e^{\frac{mb^2}{2}}\left(1-\frac{m}{b}\left(\frac{a}{b}\right)^{m-1}\right)}\,. \quad (17)$$

We introduce the following non-dimensional components as

$$R=\frac{r}{b};\quad R_0=\frac{a}{b};\quad \sigma_{rr}=\frac{T_{rr}}{Y};\quad \sigma_{\theta\theta}=\frac{T_{\theta\theta}}{Y};\quad p_i=\frac{p}{Y};\quad p_f=\frac{p}{Y_1};\quad \Omega=\frac{\rho\omega^2R^2b^2}{Y};\quad \Omega_1=\frac{\rho b^2\omega^2}{Y_1}\,. \quad (18)$$

Transitional stresses from Eq.(11) in non-dimensional form can be expressed as

$$\sigma_{rr}=\frac{-p(3-2C_0R_0^k)e^{\frac{mb^2R^2}{2}}(3-2C_0R^k)^2}{(3-2C_0R^k)^3e^{\frac{mb^2R^2}{2}}-n(3-2C_0)^3e^{\frac{mb^2}{2}}}+\frac{pn(3-2C_0)^3e^{\frac{mb^2}{2}}}{(3-2C_0R^k)^3e^{\frac{mb^2R^2}{2}}-n(3-2C_0)^3e^{\frac{mb^2}{2}}},\quad \sigma_{\theta\theta}=\frac{-m}{b}R^{m-1}\times$$

$$\times\frac{-p(3-2C_0R_0^k)e^{\frac{mb^2R_0^2}{2}}(3-2C_0R^k)^2+pn(3-2C_0)^3e^{\frac{mb^2}{2}}+p(3-2C_0R_0^k)be^{\frac{mb^2R_0^2}{2}}(3-2C_0R^k)\left[(3-2C_0R^k)mRb-\frac{4C_0kR^{k-1}}{b}\right]}{(3-2C_0R^k)^3e^{\frac{mb^2R_0^2}{2}}-n(3-2C_0)^3e^{\frac{mb^2}{2}}}-$$

$$-\frac{2p(3-2C_0R_0^k)n(3-2C_0)^3e^{\frac{mb^2}{2}}C_0k(R)^{k-1}}{\left[(3-2C_0R^k)^3e^{\frac{mb^2R_0^2}{2}}-n(3-2C_0)^3e^{\frac{mb^2}{2}}\right]b(3-2C_0R^k)^2}+\Omega\,. \quad (19)$$

Necessary pressure required for initial yielding in non-dimensional form from Eq.(14) can be written as

$$p_i=\frac{\left[(3-2C_0R_0^k)^3e^{\frac{mb^2R_0^2}{2}}-n(3-2C_0)^3e^{\frac{mb^2}{2}}\right](1+\Omega)}{(3-2C_0R_0^k)^3e^{\frac{mb^2R_0^2}{2}}\left(1-mbR_0-\frac{m}{b}R_0^{m-1}+\frac{4C_0\frac{k}{b}R_0^{k-1}}{3-2C_0R_0^k}\right)+(3-2C_0)^3e^{\frac{mb^2}{2}}\left(1-\frac{m}{b}R_0^{m-1}-\frac{2C_0\frac{k}{b}R_0^{k-1}}{3-2C_0R_0^k}\right)} \quad (20)$$

Fully plastic stresses are obtained from Eq.(19) by taking $C_0 \to 0$ in non-dimensional form as

$$\sigma_{rr} = \frac{pn\left(e^{\frac{mb^2}{2}} - e^{\frac{mb^2R^2}{2}}\right)}{e^{\frac{mb^2R^2}{2}} - ne^{\frac{mb^2}{2}}}, \tag{21}$$

$$\sigma_{\theta\theta} = \frac{-m}{b}R^{m-1}\left[\frac{pne^{\frac{mb^2}{2}} - pe^{\frac{mb^2R^2}{2}} + pb^2e^{\frac{mb^2R^2}{2}}mR}{e^{\frac{mb^2R^2}{2}} - ne^{\frac{mb^2}{2}}}\right] + \Omega .$$

Pressure required for fully plastic state in non-dimensional form from Eq.(17) can be written as

$$p_f = \frac{\left(e^{\frac{mb^2R_0^2}{2}} - ne^{\frac{mb^2}{2}}\right)(1+\Omega_1)}{e^{\frac{mb^2R_0^2}{2}}\left(1 - mR_0b - \frac{m}{b}R_0^{m-1}\right) - e^{\frac{mb^2}{2}}\left(1 - \frac{m}{b}R_0^{m-1}\right)}. \tag{22}$$

NUMERICAL DISCUSSION

In order to observe the effect of pressure on initial yielding and fully plastic state at various radii ratios, Fig. 1-8 have been drawn for thin rotating disc with variable thickness $h = h_0 e^{-(r/b)^m}$.

It is observed from Fig. 1 that at n = 1, the pressure necessary for initial yielding is maximum at centre of the disk and decreases with increasing radii ratio. Also, it is observed that effective pressure required for initial yielding decreases with the increase in non-homogeneity, for m = 1 and 2. From Figs. 2 and 3 it can be observed that pressure required for initial yielding is maximum at the centre and decreases with the increasing value of radius. With the increase in angular velocity, the pressure for initial yielding increases, as can be seen from Figs. 4-6. From Fig. 7, it can be seen that pressure for fully plastic state increases with increasing value of n, and increases with the decrease in disk thickness. The pressure required for fully plastic state attains its maximum value at m = 3. Also, the pressure for fully plastic state increases with the increase in angular velocity Ω, as can be observed from Fig. 8.

Figures 9 to 14 have been drawn between transitional circumferential stresses and different radii ratios. Circumferential stresses show increase with increasing radii ratio and attain maximum value at outer surface of the rotating disk for angular velocity (Ω = 10). Also these stresses show increase with increasing value of n as observed from Figs. 9 -11. From Figs. 12-14 it is noticed that the circumferential stresses increase with increasing value of angular velocity (Ω = 20) and attain their maximum at the outer surface of the disk. It is also observed that circumferential stresses decrease with increase in the factor of non-homogeneity and are minimum at (k = 5). Also, there is an increase in the value of circumferential stresses with decrease in thickness of the disk, as noticed from Figs. 12-14.

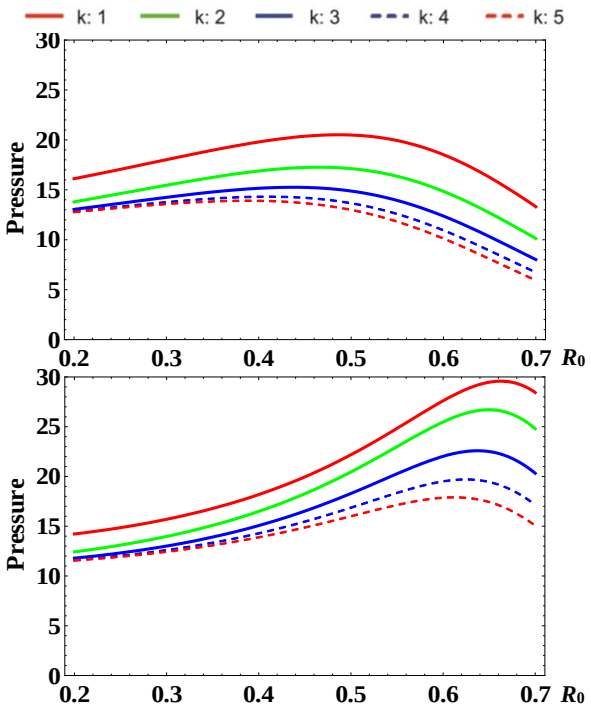

Figure 1. Effective pressure required for initial yielding with n = 1; m = 2, 3; Ω = 10.

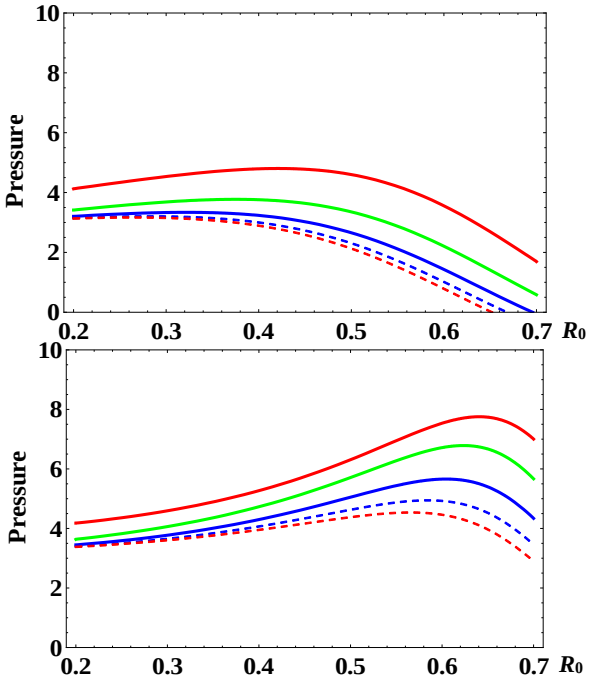

Figure 2. Effective pressure required for initial yielding with n = 0.3; m = 2, 3; Ω = 10.

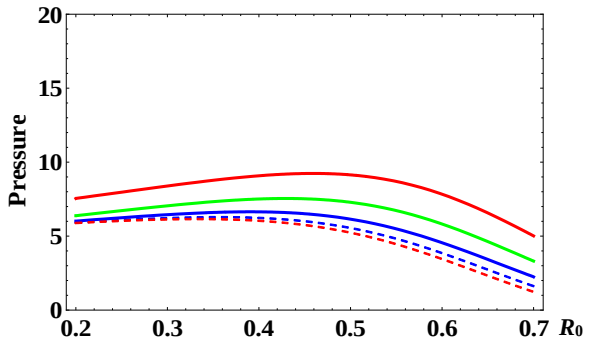

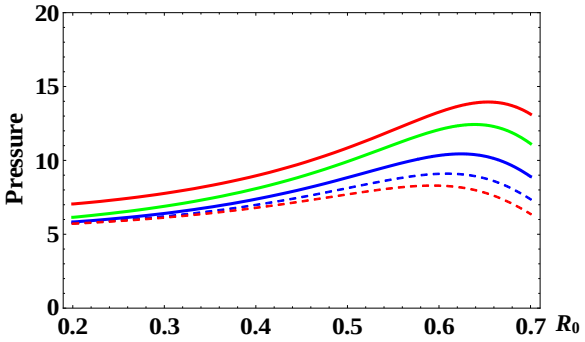

Figure 3. Effective pressure required for initial yielding with $n = 0.5$; $m = 2, 3$; $\Omega = 10$.

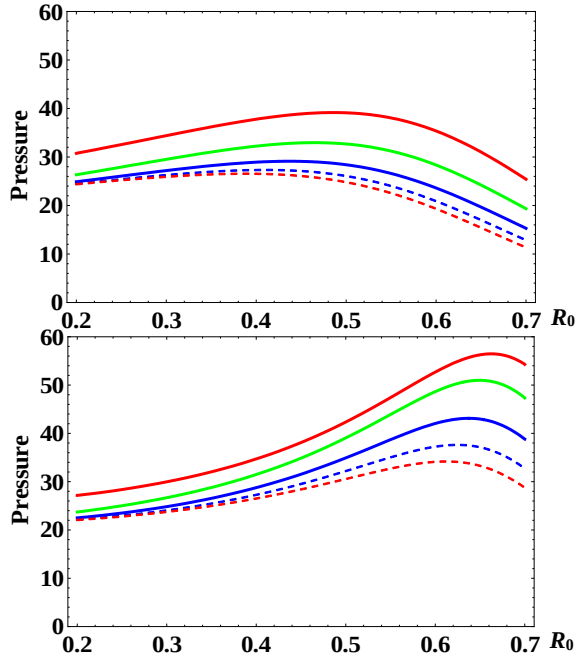

Figure 4. Effective pressure required for initial yielding with $n = 1$; $m = 2, 3$; $\Omega = 20$.

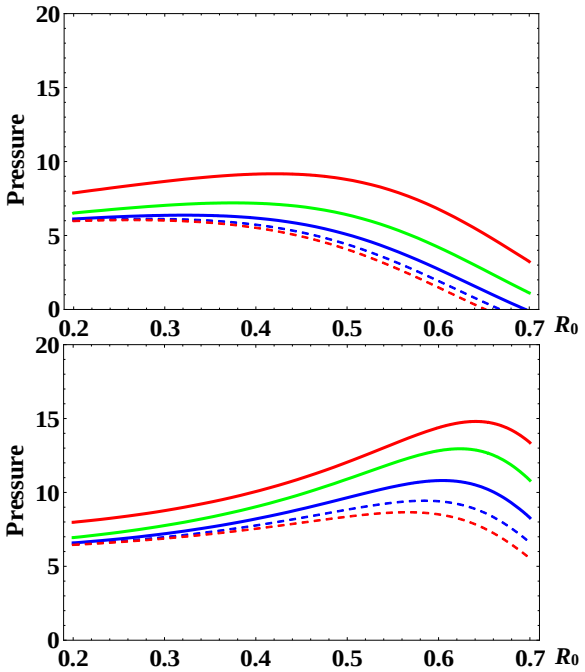

Figure 5. Effective pressure required for initial yielding with $n = 0.3$; $m = 2, 3$; $\Omega = 20$.

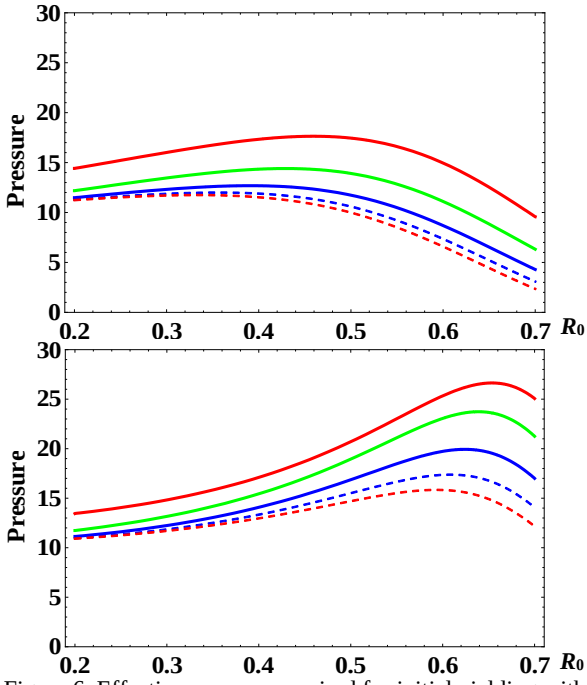

Figure 6. Effective pressure required for initial yielding with $n = 0.5$; $m = 2, 3$; $\Omega = 20$.

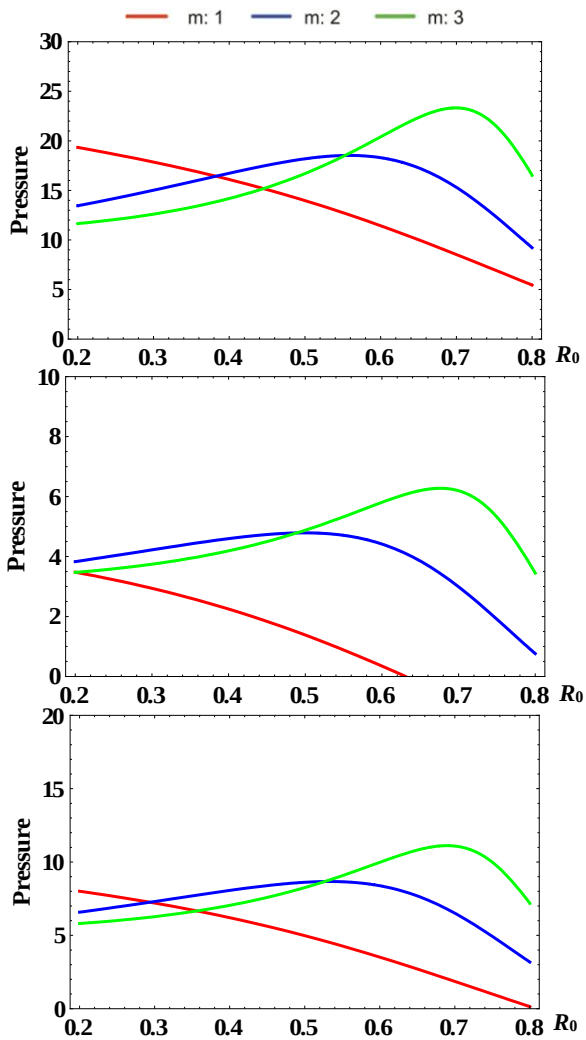

Figure 7. Effective pressure required for initial yielding with $n = 1, 0.3, 0.5$; $m = 1, 2, 3$; $\Omega = 10$.

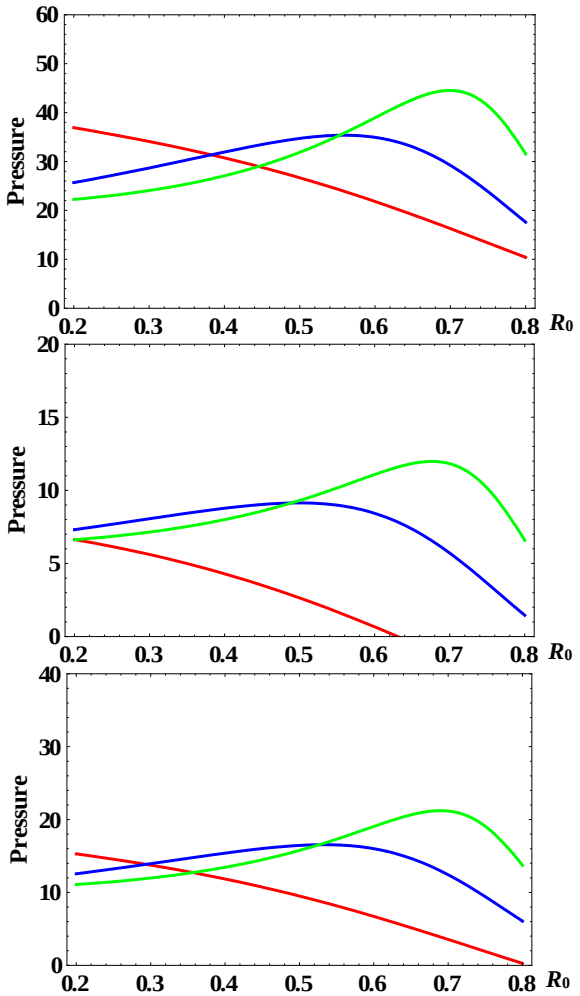

Figure 8. Effective pressure required for initial yielding with n = 1, 0.3, 0.5; m = 2, 3; Ω = 20.

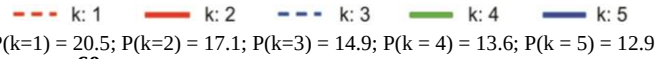

P(k=1) = 20.5; P(k=2) = 17.1; P(k=3) = 14.9; P(k = 4) = 13.6; P(k = 5) = 12.9

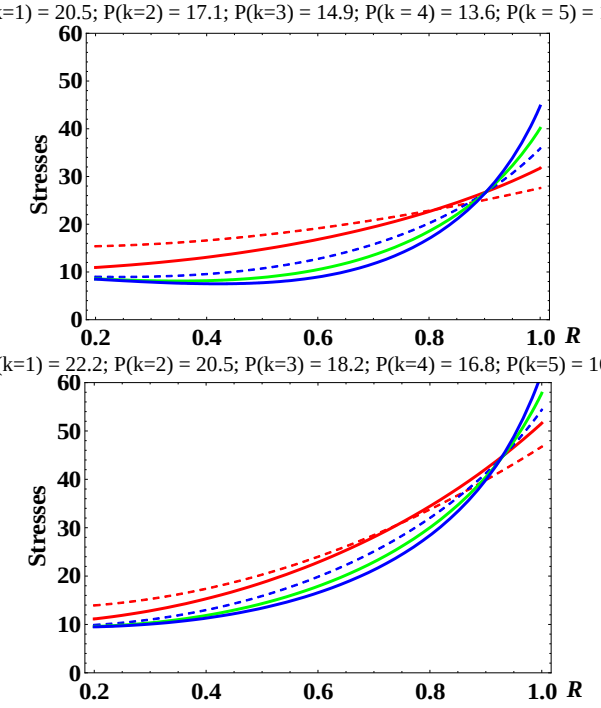

P(k=1) = 22.2; P(k=2) = 20.5; P(k=3) = 18.2; P(k=4) = 16.8; P(k=5) = 16.0

Figure 9. Transitional stresses for internal pressure and n = 1; m = 2, 3; Ω = 10.

P(k=1) = 4.6; P(k=2) = 3.4; P(k=3) = 2.65; P(k=4) = 2.3; P(k=5) = 2.1

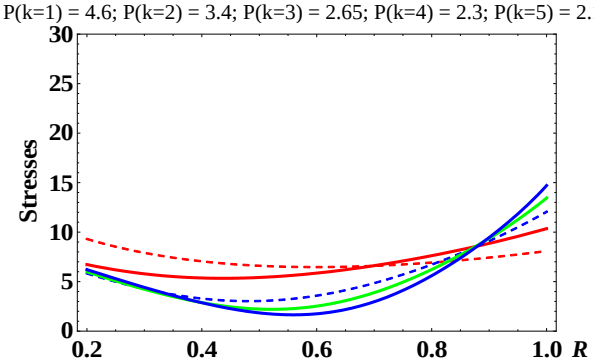

P(k=1) = 6.3; P(k=2) = 5.7; P(k=3) = 5.05; P(k=4) = 4.6; P(k=5) = 4.3

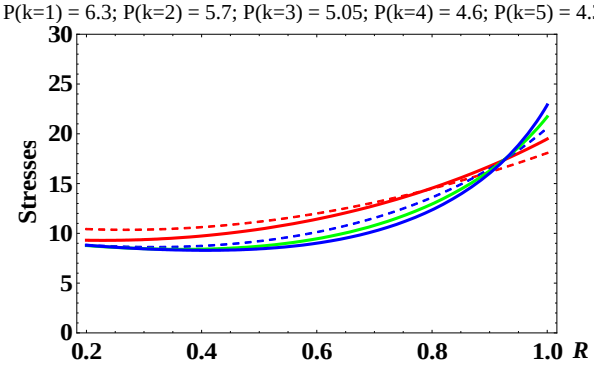

Figure 10. Transitional stresses for internal pressure and n = 0.3; m = 2, 3; Ω = 10.

P(k=1) = 9.1; P(k=2) = 7.28; P(k=3) = 6.14; P(k=4) = 5.5; P(k=5) = 5.2

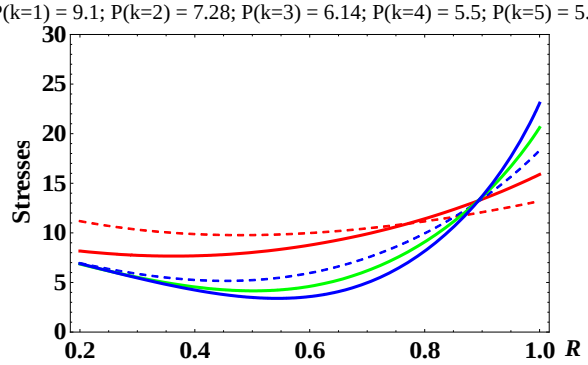

P(k=1) = 10.8; P(k=2) = 9.9; P(k=3) = 8.8; P(k=4) = 8.1; P(k=5) = 7.7

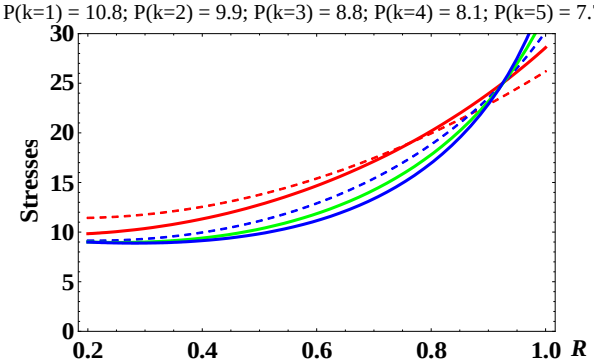

Figure 11. Transitional stresses for internal pressure and n = 0.5; m = 2, 3; Ω = 10.

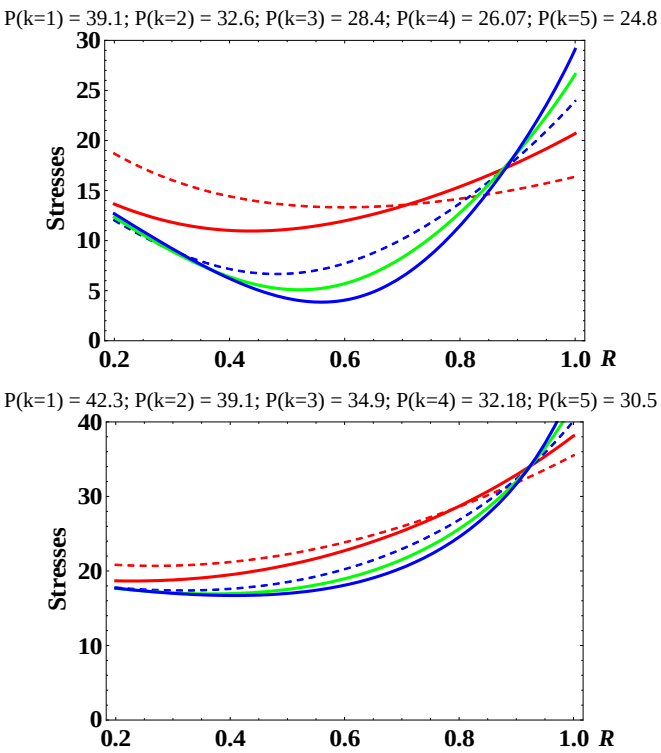

Figure 12. Transitional stresses for internal pressure and $n = 1$; $m = 2, 3$; $\Omega = 20$.

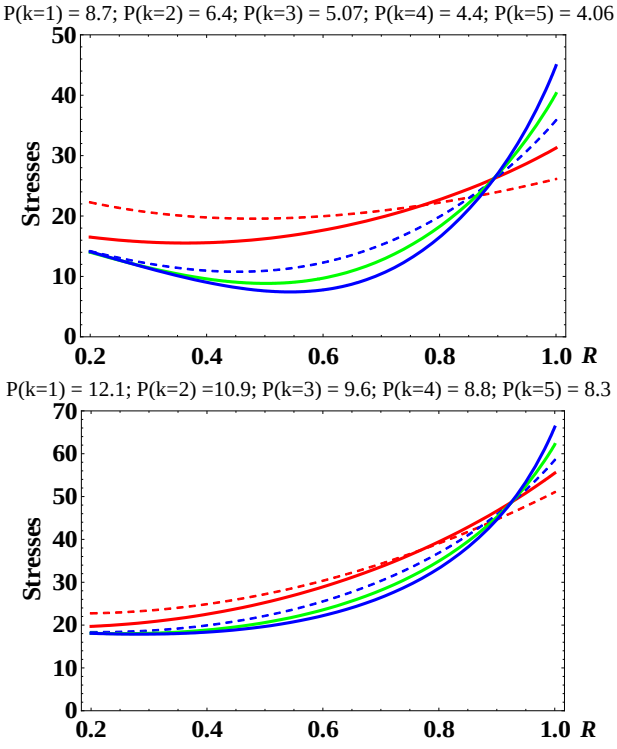

Figure 13. Transitional stresses for internal pressure and $n = 0.3$; $m = 2, 3$; $\Omega = 20$.

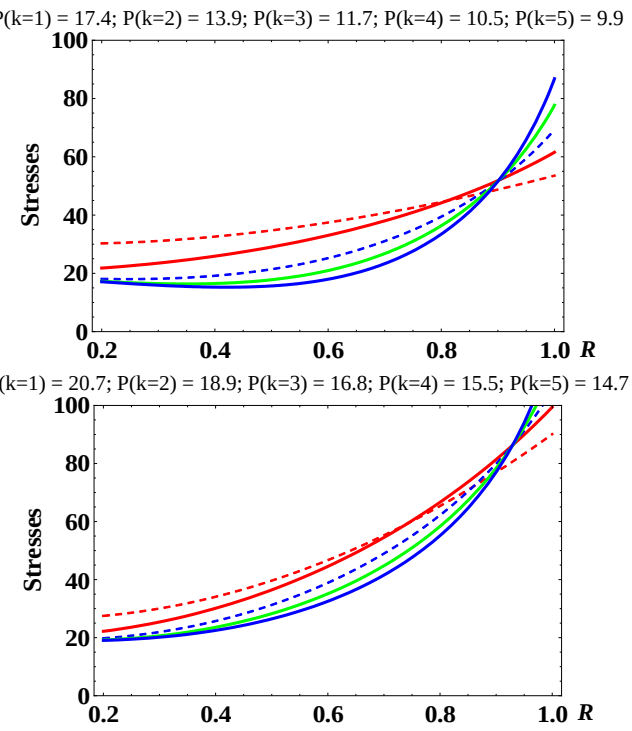

Figure 14. Transitional stresses for internal pressure and $n = 0.5$; $m = 2, 3$; $\Omega = 20$.

Figures 15 and 16 show the variation of fully plastic stresses with increasing value of radius. On the basis of graphs of fully plastic stresses, it is predicted that stresses show increase with increasing radii ratios and maximum at the outer surface of the disk. It is also noticed that fully plastic stresses have greater value at thickness parameter $m = 1$ and a minimum value at $m = 3$. Stresses in fully plastic state decrease with increase in thickness of the disk.

CONCLUSION

In this paper, the analytical method is used to solve the differential equation representing functionally graded thin rotating disk of exponentially variable thickness. The concept of transition theory is applied to evaluate the stresses in the rotating disk of functionally graded material. On the basis of all calculations and graphs, it is concluded that variable thickness and non-homogeneity have significant effects on the circumferential stresses in the rotating disk.

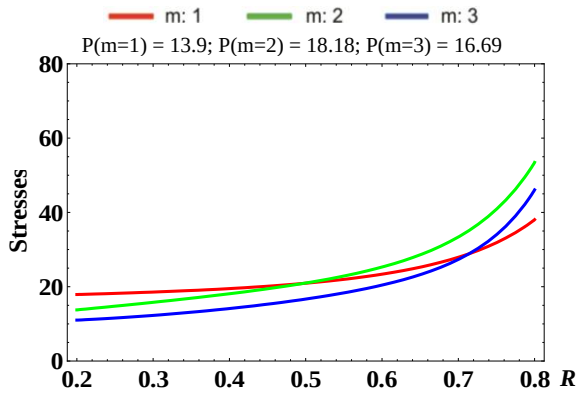

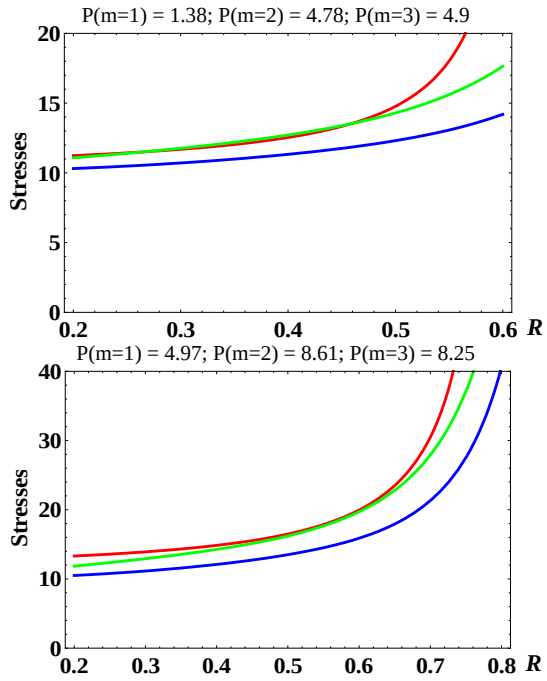

Figure 15. Fully plastic stresses with internal pressure and n = 1, 0.3, 0.5; m = 1, 2, 3; Ω = 10.

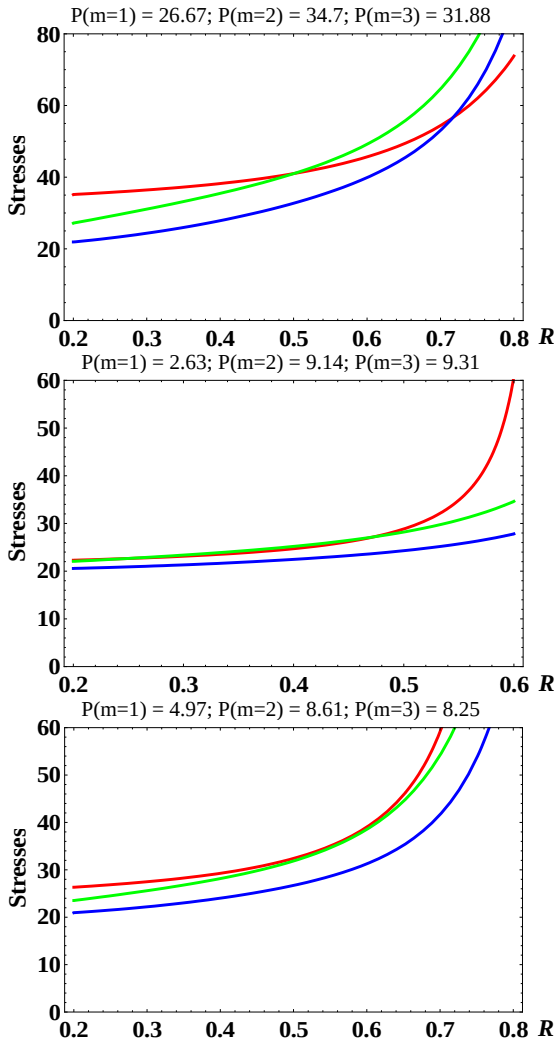

Figure 16. Fully plastic stresses with internal pressure and n = 1, 0.3, 0.5; m = 1, 2, 3; Ω = 20.

REFERENCES

1. Çallioğlu, H., Bektaş, N.B., Sayer, M. (2011), *Stress analysis of functionally graded rotating discs: analytical and numerical solutions*, Acta Mech. Sinica, 27(6): 950-955. doi: 10.1007/s10409-011-0499-8
2. Sharma, J.N., Sharma, D., Kumar, S. (2012), *Stress and strain analysis of rotating FGM thermoelastic circular disk by using FEM*, Int. J Pure & Appl. Math. 74(3): 339-352.
3. Kermani, I.D., Mirdamadi, H.R., Ghayour, M. (2014), *Nonlinear stability analysis of rotational dynamics and transversal vibrations of annular circular thin plates functionally graded in radial direction by differential quadrature*, J Vibration and Control, 22(10): 2482-2502. doi: 10.1177/1077546314547530
4. Zafarmand, H., Hassani, B. (2014), *Analysis of two-dimensional functionally graded rotating thick disks with variable thickness*, Acta Mechanica, 225(2): 453-464. doi: 10.1007/s00707-013-0966-3
5. Vivio, F., Vullo, V., Cifani, P. (2014), *Theoretical stress analysis of rotating hyperbolic disk without singularities subjected to thermal load*, J Therm. Stresses, 37(2): 117-136. doi: 10.1080/01495739.2013.839526
6. Rosyid, A., Saheb, M.E., Yahia, F.B. (2014), *Stress analysis of nonhomogeneous rotating disc with arbitrarily variable thickness using finite element method*, Res. J Appl. Sci., Eng. Tech., 7(15): 3114-3125.
7. Kouchakzadeh, M.A., Entezari, A. (2015), *Analytical solution of classic coupled thermoelasticity problem in a rotating disk*, J Therm. Stresses, 38(11): 1269-1291. doi: 10.1080/01495739.2015.1073529
8. Carrera, E., Entezari, A., Filippi, M., Kouchakzadeh, M.A. (2016), *3D thermoelastic analysis of rotating disks having arbitrary profile based on a variable kinematic 1D finite element method*, J Therm. Stresses, 39(12): 1572-1587. doi: 10.1080/01495739.2016.1207119
9. Entezari, A., Kouchakzadeh, M.A. (2016), *Analytical solution of generalized coupled thermoelasticity problem in a rotating disk subjected to thermal and mechanical shock loads*, J Therm. Stress. 39(12):1588-1609. doi: 10.1080/01495739.2016.1221329
10. Shahriari, B., Jalali, M., Ravari, M.K. (2017), *Vibration analysis of a rotating variable thickness bladed disk for aircraft gas turbine engine using generalized differential quadrature method*, in Proc. of the Inst. of Mech. Eng., Part G: J Aerospace Eng. 231(14): 2739-2749. doi: 10.1177/0954410016684360
11. Jalali, M.H., Shahriari, B., Zargar, O. (2017), *Free vibration analysis of rotating functionally graded annular disc of variable thickness using generalized differential quadrature method*, Scientia Iranica, Trans. Mech. Eng. (B), 25(2): 728-740. doi: 10.24200/sci.2017.4325
12. Gupta, S.K., Sharma, S., Pathak, S. (2000), *Creep transition in a thin rotating disc having variable thickness and variable density*, Indian J Pure Appl. Math. 31(10): 1235-1248.
13. Borah, B.N. (2005), *Thermo-elastic-plastic transition*, Contemp. Math. 379: 93-111. doi: 10.1090/conm/379/07027
14. Sharma, S., Sahni, M. (2009), *Elastic-plastic transition of transversely isotropic thin rotating disc*, Contemp. Eng. Sci. 2(9): 433-440.
15. Aggarwal, A.K., Sharma, R., Sharma, S. (2013), *Safety analysis using Lebesgue strain measure of thick-walled cylinder for functionally graded material under internal and external pressure*, The Scient. World J, 2013: 676190. doi: 10.1155/2013/676190
16. Sharma, S., Sahai, I., Kumar, R. (2013), *Creep transition of a thin rotating annular disk of exponentially variable thickness with inclusion and edge load*, Procedia Engineering, 55: 348-354. doi: 10.1016/j.proeng.2013.03.264

17. Sharma S., (2017), *Creep transition in bending of functionally graded transversely isotropic rectangular plates*, Struct. Integ. and Life, 17(3): 187-192.
18. Sharma, S., Yadav, S., Sharma, R. (2017), *Thermal creep analysis of functionally graded thick-walled cylinder subjected to torsion and internal and external pressure*, J Solid Mech. 9(2): 302-318.
19. Sharma, S. (2017), *Stress analysis of elastic-plastic thick-walled cylindrical pressure vessels subjected to temperature*, Struct. Integ. and Life, 17(2): 105-112.
20. Sharma, S., Panchal, R. (2017), *Thermal creep deformation in pressurized thick-walled functionally graded rotating spherical shell*, Int. J Pure & Appl. Math. 114(3): 435-444. doi: 10.12732/ijpam.v114i3.2
21. Sharma, S., Sharma, R., Panchal, R. (2018), *Creep transition in transversely isotropic composite circular cylinder subjected to internal pressure*, Int. J Pure & Appl. Math. 120(1), 87-96. doi: 10.12732/ijpam.v120i1.8
22. Sharma, S., Yadav, S., Sharma, R. (2018), *Creep torsion in thick-walled circular cylinder under internal and external pressure*, Struct. Integ. and Life, 18(2): 89-97.
23. Sharma, S., Panchal, R. (2018), *Creep stresses in functionally graded rotating orthotropic cylinder with varying thickness and density under internal and external pressure*, Struct. Integ. and Life, 18(2): 111-119.
24. Yadav, S., Sharma, S. (2018), *Torsion in microstructure hollow thick-walled circular cylinder made up of orthotropic material*, J Solid Mech. 10(3): 581-590.
25. Sharma, S., Panchal, R. (2018), *Elastic-plastic transition of pressurized functionally graded orthotropic cylinder using Seth's transition theory*, J Solid Mech. 10(2): 450-463.
26. Sharma, R., Sharma, S., Radaković, Z. (2018), *Thermal creep analysis of pressurized thick-walled cylindrical vessels*, Structural Integrity and Life, 18(1): 7-14.
27. Sharma, S., Yadav, S., Radaković, Z. (2018), *Finite creep deformation in thick-walled circular cylinder with varying compressibility under external pressure*, Struct. Integrity and Life, 18(1): 31-36.
28. Sharma, S., Yadav, S. (2019), *Numerical solution of thermal elastic-plastic functionally graded thin rotating disk with exponentially variable thickness and variable density*, Therm. Sci. 23(1): 125-136. doi: 10.2298/TSCI131001136S